Effective Dielectric Constants of Mixed-Phase Hydrometeors

R. MENEGHINI

NASA Goddard Space Flight Center, Greenbelt, Maryland

L. LIAO

Caelum Research Company, Rockville, Maryland

(Manuscript received 7 December 1998, in final form 24 June 1999)

ABSTRACT

Melting snow, graupel, and hail are often modeled as uniform mixtures of air–ice–water or ice–water. Two-layered models have also been proposed in which the particle consists of a dry snow or ice core surrounded by water or a wet snow mixture. For both types of particle models, the mixtures are characterized by effective dielectric constants. This information, along with particle shape, size, and orientation, provides the necessary data for calculating the scattering characteristics of the particles. The most commonly used formulas for the effective dielectric constant, ε_{eff}, are those of Maxwell Garnett and Bruggeman. To understand the applicability and limitations of these formulas, an expression for ε_{eff} is derived that depends on the mean internal electric fields within each component of the mixture. Using a conjugate gradient numerical method, the calculations are carried out for ice–water mixtures. Parameterization of the results in terms of the fractional water volume and the electromagnetic wavelength provides an expression for ε_{eff} for wavelengths between 3 and 28 mm. To circumvent the laborious task of parameterizing ε_{eff} with wavelength for air–ice–water mixtures, several approximate formulations are proposed. Tests of the accuracy of the formulas are made by calculating the mean and variance from different particle realizations and by comparison to a previous method. Tests of the applicability of the formulas for ε_{eff} are made by changing the shape, size, and orientations of the inclusions. While the formulas are adequate over a certain range of inclusion sizes and for a change in shape from cubic to spherical, they are not applicable to highly eccentric, aligned inclusions such as rods or plates.

1. Introduction

Among the difficulties encountered in calculating scattering characteristics of partially melted snow or ice are the unknown distributions of shapes, sizes, orientations, and fractional water contents. Even at the level of single particle scattering questions arise with respect to the spatial distribution of water, ice, and air within the particle and the way in which this structure determines the effective dielectric constant of the mixture. Melting hydrometeors are usually modeled either as a uniform mixture of ice–water or air–ice–water or as a two-layered particle consisting of a water, wet snow, or wet ice coating about an inner core of snow or ice (Aydin and Zhao 1990; Bringi et al. 1986; Fabry and Szyrmer 1999). Once the effective dielectric constant, ε_{eff}, of the mixtures is specified the scattering characteristics are obtained either by numerical methods such as the T-matrix (Barber and Hill 1990) or, in the case of concentric spheres, by an exact solution (Aden and Kerker 1951). However, the various dielectric formulas not only yield different results but themselves depend on how the constituents are ordered. For a three-component mixture, where the fractional volumes are fixed, the Maxwell Garnett formula (Maxwell Garnett 1904; Bohren and Battan 1980, 1982) admits 12 possible solutions and the Bruggeman, or effective medium formula (Bruggeman 1935), provides 3 solutions.

In an attempt to improve upon the dielectric formulas for ice–water and air–ice–water mixtures, we begin with the definition of the effective dielectric constant and, following Stroud and Pan (1978), derive an expression for ε_{eff} as a function of the mean values of the internal fields. The internal fields are computed by means of the conjugate gradient numerical method and then parameterized as functions of the electromagnetic wavelength and the fractional volumes of the constituents. In the first part of the paper, an expression is given for ε_{eff} for an ice–water mixture. As this formula depends only on the ratio of the mean fields in the two materials, the focus of the numerical analysis is to compute this ratio as a function of fractional water volume f and wavelength λ. A parameterization in f and λ (from 3 to 28

Corresponding author address: Dr. Bob Meneghini, Code 975, NASA GSFC, Greenbelt, MD 20771.
E-mail: bob@priam.gsfc.nasa.gov

mm) provides a relatively simple expression for ε_{eff}. For a three-component mixture of ice, air, and water, the numerical computations needed to express the results as functions of wavelength and volume fractions are more demanding. Approximate methods, based on the results for two-component mixtures, are investigated and compared to the direct numerical calculations for several cases. To test the accuracy and applicability of the formulas, the effects of shape, size, and orientation of the inclusions are investigated. The present formulation is also compared to an earlier approach (Meneghini and Liao 1996).

2. Derivation of ε_{eff}

If the materials that make up the particle are homogeneous, isotropic, and linear, the effective dielectric constant, ε_{eff}, for a mixture at free-space wavelength λ, can be defined by the equation (Stroud and Pan 1978; Chylek et al. 1991)

$$\varepsilon_{\text{eff}} \int \mathbf{E}(\mathbf{x}, \lambda)\, dV = \int \mathbf{D}(\mathbf{x}, \lambda)\, dV, \tag{1}$$

where $\mathbf{E}$ is the electric field vector and $\mathbf{D}$ is the electric displacement vector and where the integrals of (1) are taken over the volume of the particle. Letting the integrals be approximated by summations of the integrands evaluated at the center of small equivolume elements comprising the particle, then on writing $\mathbf{D}_j = \varepsilon_j \mathbf{E}_j$ at the jth element, (1) can be expressed as

$$\sum (\varepsilon_j - \varepsilon_{\text{eff}}) E_j = 0 \tag{2}$$

for each vector component of the field. For a mixture consisting of two materials, ε_j assumes the value either of the dielectric constant of material 1 (ε_1) or of material 2 (ε_2) so that (2) can be written

$$\varepsilon_1 \sum_{j \in M_1} E_j + \varepsilon_2 \sum_{j \in M_2} E_j = \varepsilon_{\text{eff}} \left(\sum_{j \in M_1} E_j + \sum_{j \in M_2} E_j \right), \tag{3}$$

where the notation $\Sigma_{(j \in M_k)}$ denotes a summation over all volume elements comprising the kth component of the mixture ($k = 1, 2$). Passing to the limit of a large number of elements, keeping the volume fractions of the components fixed, $\Sigma_{(j \in M_k)} E_j$ is replaced by $N_k \langle E_k \rangle$, where N_k is the number of elements comprising the kth material and $\langle E_k \rangle$ is the corresponding mean field. Dividing by the total number of elements, N, and letting $f_k\ (= N_k/N)$ be the fractional volume of component k, (3) can be expressed in the form

$$\varepsilon_{\text{eff}} = \frac{[\varepsilon_1 f_1 \langle E_1 \rangle + \varepsilon_2 f_2 \langle E_2 \rangle]}{[f_1 \langle E_1 \rangle + f_2 \langle E_2 \rangle]}, \tag{4}$$

where $f_1 + f_2 = 1$. Equation (4) can be rewritten

$$\varepsilon_{\text{eff}} = \left[\varepsilon_1 f_1 \left(\frac{\langle E_1 \rangle}{\langle E_2 \rangle} \right) + \varepsilon_2 f_2 \right] \Bigg/ \left[f_1 \left(\frac{\langle E_1 \rangle}{\langle E_2 \rangle} \right) + f_2 \right], \tag{5}$$

so that ε_{eff} can be computed if the ratio of the mean fields in the two materials, $\langle E_1 \rangle / \langle E_2 \rangle$, is known. An identical argument yields ε_{eff} for an N component mixture

$$\varepsilon_{\text{eff}} = [\varepsilon_1 f_1 \langle E_1 \rangle + \cdots + \varepsilon_N f_N \langle E_N \rangle] \div [f_1 \langle E_1 \rangle + \cdots + f_N \langle E_N \rangle], \tag{6}$$

where $f_1 + \cdots + f_N = 1$. Equation (6) will be used later in computing the effective dielectric constant for mixtures of ice, air, and water. Stroud and Pan (1978) use an alternative, but equivalent, expression to compute ε_{eff} by relating the internal electric fields to the forward scattering amplitude. Generalizations and applications of these extended effective medium (EEM) formulas can be found in several papers (Stroud 1975; Chylek and Srivastava 1983; Chylek et al. 1988, 1991; Videen and Chylek 1994). Stroud and Pan (1978) and Chylek and Srivastava (1983) show that the Maxwell Garnett and Bruggeman formulas can be derived as special cases of the EEM formulation. In this and in a previous paper (Meneghini and Liao 1996) the conjugate gradient method is used to compute the internal fields. Other numerical methods that have been used include the finite element formulation of Laplace's equation and the boundary integral equation for two- and three-dimensional geometries (Boudida et al. 1998; Sareni et al. 1997a,b) as well as a volume integral method for a one-dimensional composite layer (Pincemin and Greffet 1994).

3. Calculations of ε_{eff}

a. Preliminary remarks

According to (5), the effective dielectric constant of a two-component mixture can be computed once the ratio of the mean fields in the two materials is known. This calculation requires, in turn, a particle model and a means by which the internal fields can be computed. In this paper, the conjugate gradient–fast Fourier transform (CG–FFT) method is used for the field calculation. Descriptions and applications of the method can be found in the literature (Catedra et al. 1995; Sarkar et al. 1986; Su 1989). Each particle is divided into 32^3 equivolume cubic elements, and the elements are arranged so the particle itself is cubic. In computing the internal fields, the particle size is taken to be electrically small: letting L^3 be the particle volume and a the radius of an equivolume sphere, the size parameter $2\pi a/\lambda$ is taken to be 0.1. Comparisons of ε_{eff} derived from size parameters up to 1 are in good agreement; these results will be discussed later in the paper. The continuity requirement of the tangential electric field E_t, and the normal electric displacement D_n, at the interfaces between materials 1 and 2, implies that the minimum size of inclusion (and matrix) material must be larger than the elements into which the particle is divided. To reduce the influence of these errors, the smallest size of any region of material 1 or 2 is taken to consist of 4^3 cubic elements.

Effects of the size and shape of the inclusions will be considered later in the paper.

In calculating the internal fields, an x-polarized incident electric field is assumed to propagate in the z direction. As with all examples that will be considered in this paper, the distribution of the components of the mixture are assumed to be spatially uniform (random) in the sense that the probability that a particular material is present at any cell (consisting of either 4^3 or 8^3 cubic elements) depends only on the fractional volume of the material. For example, to generate a particle with 30% water, independent random numbers, uniformly distributed between (0, 1), are selected for each of the $32^3/4^3$ (512) or $32^3/8^3$ (64) subdomains that comprise the particle. If the random number is less than 0.3, the region is taken to be water, otherwise it is taken to be ice. A realization of an ice–water particle consisting of 50% water and 50% ice is shown in Fig. 1, where a cross section of the particle is shown in the x–y plane. Shaded regions represent water. In this example, any region of either ice or water consists of at least 4^3 cubic elements. Phasor representations of E_x and D_x for an incident wavelength of 8.6 mm (35 GHz) are also shown in Fig. 1 at each of the 32×32 elements. Note that the origin of the phasor, represented by an arrow, begins at the lower left-hand corner of each element. Electric field strength is proportional to the length of the arrow and the phase is represented by the direction, where phases of 0° and 90° correspond to x- and y-directed arrows, respectively. For the fields shown in Fig. 1, the relevant continuity checks are the equality of the E_x phasors at the ice–water interfaces in the y = constant planes (lines) and the equality of the D_x phasors at the interfaces in the x = constant planes (lines).

The relationship between particles with inclusion sizes consisting of 4^3 and 8^3 cubic elements can be seen from a comparison of Figs. 1 and 2, where the fractional water contents are the same in both cases but where the minimum inclusion size for the particle shown in Fig. 2 is 8^3 elements. As will be shown later, comparisons between the ε_{eff} deduced from the two-particle representations are approximately the same; that is, ε_{eff} is relatively insensitive to the size of inclusions over this size range. For the results given in following section, the minimum region size is assumed to be composed of 4^3 cubic elements.

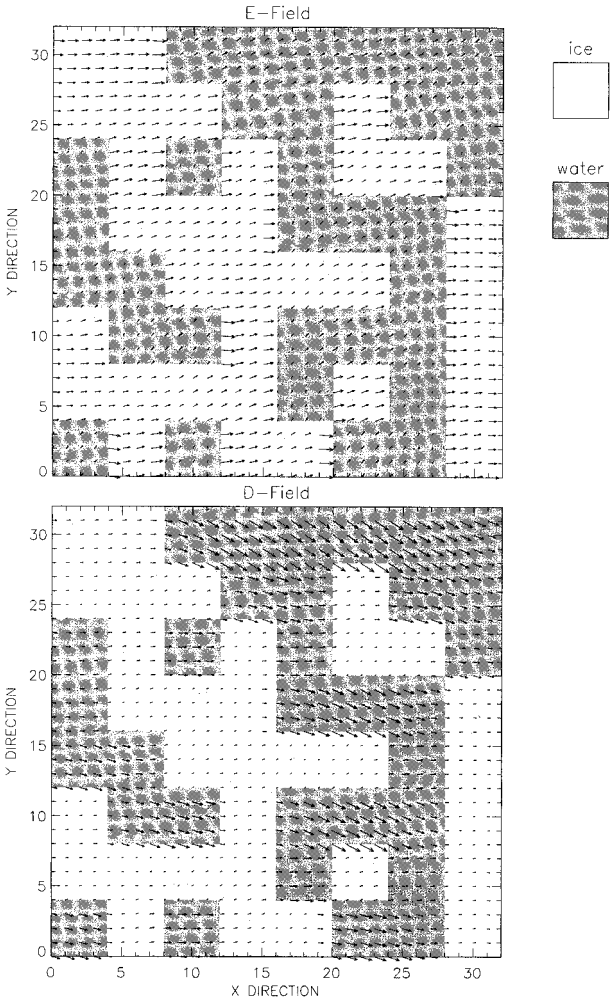

FIG. 1. Two-dimensional cut through a realization of a cubic particle composed of a water–ice mixture of equal fractional volumes. Arrows at each of the 32×32 elements show the phasor representation of the x components of the **E** and **D** fields for an incident x-directed **E** field propagating in the z direction. Minimum size of water and ice regions consists of $4 \times 4 \times 4$ elements.

b. Numerical results for ice–water mixtures

Equation (5) implies that ε_{eff} can be determined once the ratio of fields in the two materials, $\langle E_1 \rangle / \langle E_2 \rangle$, is known. Plots of the real (top) and imaginary (bottom) parts of this ratio for an water–ice mixture, $\langle E_w \rangle / \langle E_i \rangle$, are shown in Fig. 3 as a function of the fractional water volume for the Special Sensor Microwave/Imager (SSM/I) wavelengths, λ, of 15.5, 8.6, and 3.5 mm (frequencies of 19.35, 35, and 85 GHz). A fractional water volume of 0 corresponds to a pure ice particle. The results suggest that for a fixed wavelength, the real and imaginary parts of the ratio $\langle E_w(f, \lambda) \rangle / \langle E_i(f, \lambda) \rangle$ can be approximated by a linear function in the volumetric water fraction, f:

$$\text{Re}[\langle E_w(f, \lambda) \rangle / \langle E_i(f, \lambda) \rangle] = A_r(\lambda) f + B_r(\lambda) \quad \text{and} \quad (7)$$

$$\text{Im}[\langle E_w(f, \lambda) \rangle / \langle E_i(f, \lambda) \rangle] = A_i(\lambda) f + B_i(\lambda), \quad (8)$$

where the coefficients $A_r(\lambda)$, $B_r(\lambda)$, $A_i(\lambda)$, and $B_i(\lambda)$ are found for each wavelength by a linear regression. As a test of (7) and (8), let $\lambda = 15.5$ mm (19.35 GHz); inserting the values of $\langle E_w(f, \lambda = 15.5) \rangle / \langle E_i(f, \lambda = 15.5) \rangle$, as shown in Fig. 3, into (5) yields $\varepsilon_{\text{eff}}(f, \lambda = 15.5)$ for water fractions $f = 0.05, 0.1, \ldots, 0.95$. The results, represented by the solid circles, are shown in the complex plane in Fig. 4 where the top-right-most point corresponds to $f = 0.95$, and the bottom-left-most

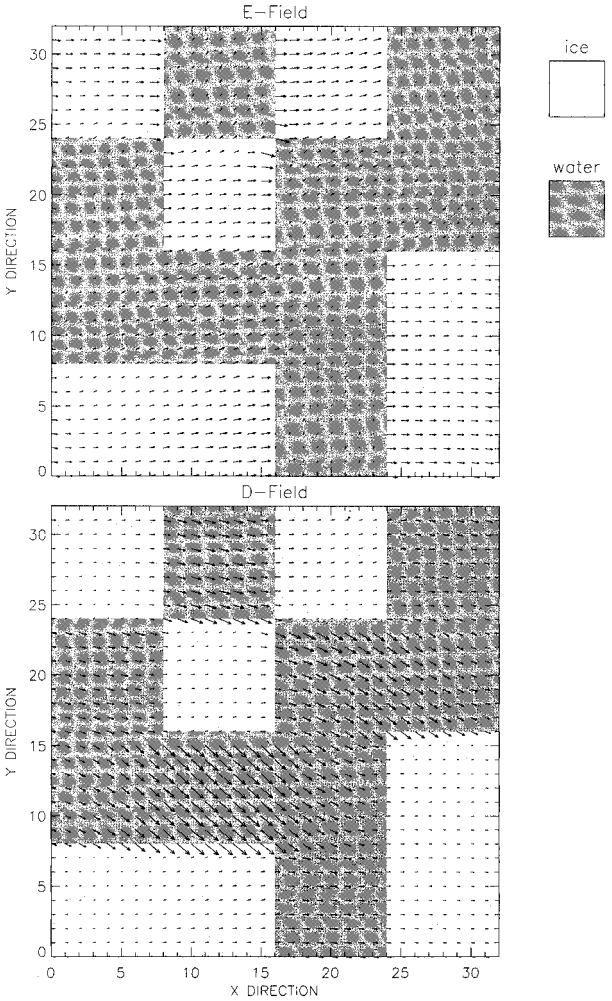

FIG. 2. Same as Fig. 1 but where the minimum size of the water and ice regions consists of $8 \times 8 \times 8$ elements.

point corresponds to $f = 0.05$. Note that for pure ice ($f = 0$) and pure water ($f = 1$) (5) reduces to the dielectric constants of ice and water, respectively. Values of ε_{eff}, derived from (5), using the linear approximations of (7) and (8) for the mean field ratio, are represented by dashed lines.

Also shown in Fig. 4 are the dielectric constants derived from the Bruggeman formula (box) and from the Maxwell Garnett with water matrix–ice inclusions, MG_{wi}, (solid line with shaded triangles) and with ice matrix–water inclusions, MG_{iw} (dashed line with open triangles). As seen in the figure the numerical results tend to be close to the MG_{iw} solution at low fractional water contents but increasingly deviate from the MG_{iw} results as the water fraction increases. Plots (not shown) of ε_{eff} were generated for five other frequencies. As in Fig. 4, ε_{eff} derived from the linear approximations of (7) and (8) reproduce the directly calculated numerical results well. Moreover, the relationships among the numerical results and the Maxwell Garnett and Bruggeman

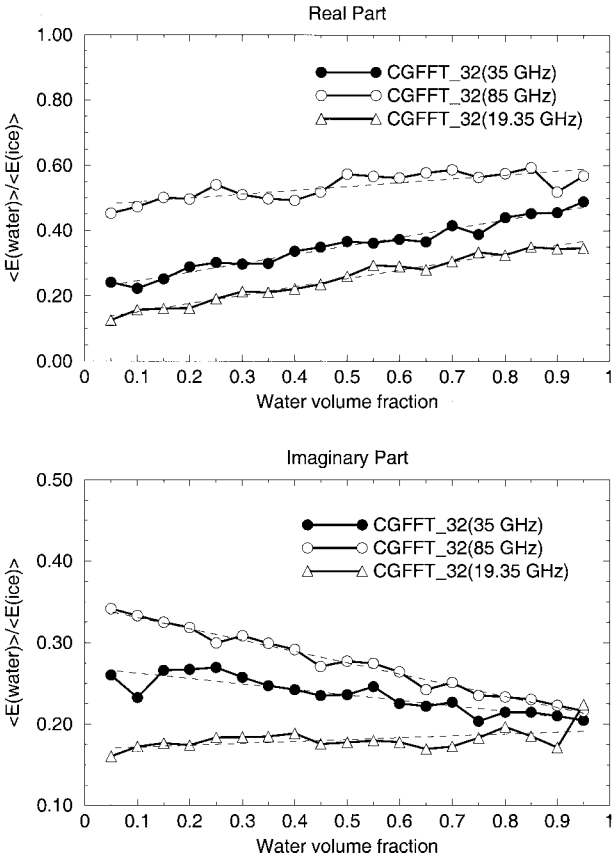

FIG. 3. Real (top) and imaginary (bottom) parts of the mean ratio of fields in water and ice as functions of the water percentage for frequencies of 19.35, 35, and 85 GHz. Straight lines through the points represent the best-fit (minimum mean-square error) values.

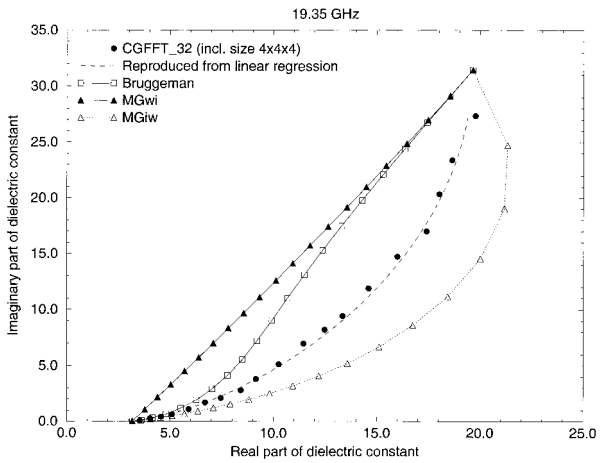

FIG. 4. Plots of the effective dielectric constant, ε_{eff}, in the complex plane at a frequency of 19.35 GHz. Results from the numerical method are represented by the solid circles for fractional water volumes of 0.05, 0.1, . . . , 0.95. An estimate of ε_{eff} as derived from the straight line approximations to $\langle E_w \rangle / \langle E_i \rangle$ are given by the dashed line. Results from the Bruggeman (solid line with squares), Maxwell Garnett, water matrix (solid line with open triangle), and Maxwell Garnett ice matrix (dashed line with shaded triangle) are shown for $f_w = 0, 0.05, \ldots, 0.95, 1$.

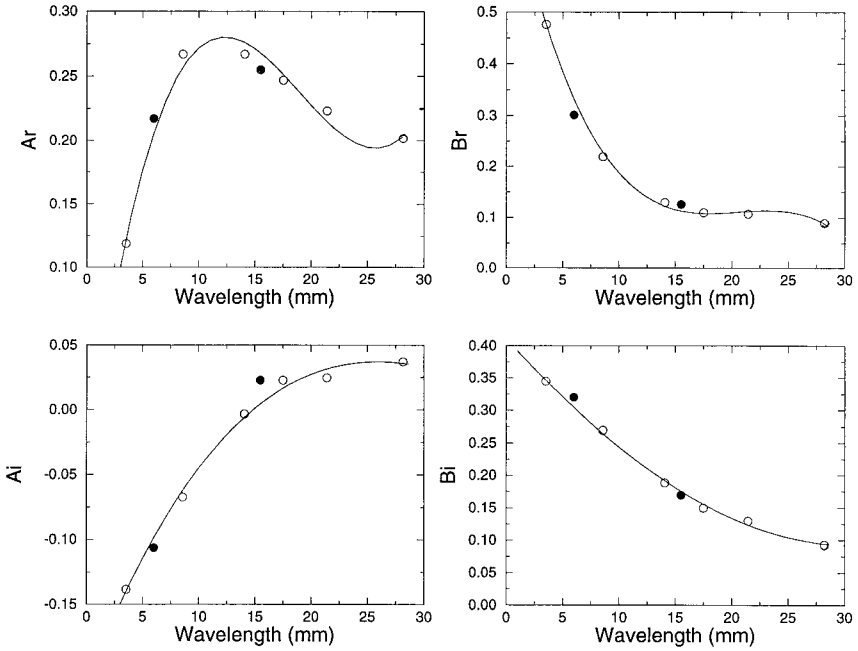

FIG 5. Least square cubic fits for the coefficients of Eqs. (7) and (8) vs wavelength for data at five wavelengths (open circles). The closed circles are used as checks on the fit and are not used in the fitting procedure.

formulations are qualitatively similar to those shown in Fig. 4.

It follows from (5), (7), and (8) that ε_{eff} can be written as a function of the fractional water content, f. To parameterize ε_{eff} in the free-space wavelength λ (mm), the coefficients $A_r(\lambda)$, $A_i(\lambda)$, $B_r(\lambda)$, and $B_i(\lambda)$ must be expressed as functions of λ. Values of these coefficients at six wavelengths are represented by the circles in Fig. 5. Writing $A_r(\lambda)$ in the form

$$A_r(\lambda) = c_0 + c_1\lambda + c_2\lambda^2 + c_3\lambda^3, \qquad (9)$$

the coefficients $c_0, \ldots, c_3$ are found by minimizing the mean square error between (9) and the six values of A_r shown in the top left panel of Fig. 5. (The two sets of points, represented by the solid circles at $\lambda = 6$ and 15.5 mm are used as checks on the fits and are not used in the calculation of the best-fit curves.) An identical procedure is used for the remaining coefficients. These approximations for $A_r(\lambda)$, $A_i(\lambda)$, $B_r(\lambda)$, and $B_i(\lambda)$ are represented by solid lines in each of the four panels of Fig. 5. Values of the coefficients are given in Table 1. Equation (5) together with (7) through (9) and the values of Table 1 constitute an approximation for the effective dielectric constant ε_{eff} for a two-component uniform mixture of ice and water as a function of the fractional water volume f and wavelength λ for 28 mm $> \lambda >$ 3 mm.

c. Three-component mixture: air, ice, and water

The formula for a three-component mixture is given by (6) with $N = 3$. This can be written in the form

$$\varepsilon_{\text{eff}} = [\varepsilon_w f_w\langle E_w\rangle/\langle E_i\rangle + \varepsilon_a f_a\langle E_a\rangle/\langle E_i\rangle + \varepsilon_i f_i] \div [f_w\langle E_w\rangle/\langle E_i\rangle + f_a\langle E_a\rangle/\langle E_i\rangle + f_i], \qquad (10)$$

where the subscripts i, w, and a denote ice, water, and air, respectively, and where $f_w + f_a + f_i = 1$. In contrast to (5) there are two unknown ratios of mean fields: those of water to ice and air to ice. In principle, the ratios of fields in (10) can be computed for all combinations f_w and f_i (where $f_a = 1 - f_i - f_w$). The task, however, is formidable. For a two-component medium, the computer time needed for 19 values of the fractional water

TABLE 1. Cubic fits for the parameters A_r, A_i, B_r, and B_i in (7) and (8) of the form $c_0 + c_1\lambda + c_2\lambda^2 + c_3\lambda^3$, where λ is the wavelength in millimeters.

	c_0	c_1	c_2	c_3
A_r	-6.97×10^{-2}	6.775×10^{-2}	-4.074×10^{-3}	7.148×10^{-5}
B_r	0.76635	-0.099	4.90×10^{-3}	-7.944×10^{-5}
A_i	-2.113×10^{-1}	2.223×10^{-2}	-6.072×10^{-4}	4.6025×10^{-6}
B_i	0.4116	-0.0193	2.365×10^{-4}	1.7503×10^{-6}

volume f at six wavelengths is approximately 350 hours on a Silicon Graphics Origin 200 computer. For a three-component medium, the calculations can be expected to increase by more than a factor of 10.

One alternative to the direct numerical calculation of (10) is the replacement of the air–ice–water mixture with a snow–water mixture of snow density ρ_s, equal to $\rho_i f_i/(f_i + f_a)$, where ρ_i is the mass density of ice (0.92 g cm^{-3}). Since this is a two-component mixture, ε_{eff} can be calculated from (5) from which ε_{eff} can be approximated as a function of f_w, λ, and ρ_s. The computational effort, however, is substantial and a simpler approximation is desirable. To explore this possibility, consider the following hypothesis: $\langle E_w\rangle/\langle E_i\rangle$ ($\langle E_a\rangle/\langle E_i\rangle$) can be approximated by the results obtained from a two-component ice–water mixture (air–ice mixture). In these approximations, the third component of the mixture is ignored so that, for example, the presence of air is assumed to have no effect on $\langle E_w\rangle/\langle E_i\rangle$. Under these assumptions, $\langle E_w\rangle/\langle E_i\rangle$, given by (7) and (8), can be used in (10). An issue of interpretation immediately arises, however. In (7) and (8), $\langle E_w\rangle/\langle E_i\rangle$ is expressed as a function of the fractional water volume, f_w, where $f_w + f_i = 1$. For a three-component mixture, however, there are two interpretations as to the meaning of f_w: either the volume of water relative to the total volume of the particle (air–ice–water), or the volume of water relative to the volume of the ice and water only. In the results presented below, the former definition is used because it compares more favorably with the numerical results. That this definition provides better accuracy may be because the fractional water volume is the most critical parameter in determining ε_{eff}, and only the former definition of f_w gives the true fractional water content of the particle.

To determine the second ratio of internal fields, $\langle E_a\rangle/\langle E_i\rangle$, the results of Debye (1929) are used, where, to a good approximation (Battan 1973),

$$K_s\rho_i = K_i\rho_s, \tag{11}$$

where ρ_i and ρ_s are the mass densities of ice and snow, respectively, and where $K_s = (\varepsilon_s - 1)/(\varepsilon_s + 2)$ and $K_i = (\varepsilon_i - 1)/(\varepsilon_i + 2)$, where ε_i and ε_s are the dielectric constants of ice and snow, respectively. Solving (11) for ε_s gives

$$\varepsilon_s = [\rho_i + 2K_i\rho_s]/[\rho_i - K_i\rho_s]. \tag{12}$$

But for an ice–air mixture, (5) yields

$$\varepsilon_{\text{eff}} = \varepsilon_s = [\varepsilon_i f_i' + \varepsilon_a f_a'(\langle E_a\rangle/\langle E_i\rangle)] \div [f_i' + f_a'(\langle E_a\rangle/\langle E_i\rangle)], \tag{13}$$

where f_i' and f_a' are the fractional volumes of the air–ice mixture and are related to the true fractional volumes f_i, f_a by $f_i' = f_i/(f_i + f_a)$ and $f_a' = f_a/(f_i + f_a)$, where $f_i' + f_a' = 1$. Solving (13) for $\langle E_a\rangle/\langle E_i\rangle$ gives

$$\langle E_a\rangle/\langle E_i\rangle = f_i'(\varepsilon_s - \varepsilon_i)/[f_a'(\varepsilon_a - \varepsilon_s)]. \tag{14}$$

Note that (14) and the approximation for $\langle E_w\rangle/\langle E_i\rangle$ given by (7) and (8), when used in (10), provide an estimate of ε_{eff} for air–ice–water mixtures for wavelengths in the range from 3 to 28 mm.

To summarize the previous discussion, recall that for a three-component mixture of air–ice–water the effective dielectric constant, defined by (10), can be calculated numerically from the mean field ratios $\langle E_w\rangle/\langle E_i\rangle$ and $\langle E_a\rangle/\langle E_i\rangle$. This set of calculations will be referred to as the direct method. The first alternative to this (approximation A) is to combine the air and ice into a snow medium so ε_{eff} can be determined from a numerical calculation of the ratio of the mean field in water to that in snow, $\langle E_w\rangle/\langle E_s\rangle$. A second alternative is to use (10) with $\langle E_w\rangle/\langle E_i\rangle$ given by (7) and (8) and $\langle E_a\rangle/\langle E_i\rangle$ determined either from (12) and (14) (approximation B_1) or from the CG–FFT results for an ice–air mixture (approximation B_2). To compare these formulations, realizations of water–ice–air mixtures are constructed by fixing the water content and varying the ratio of ice and air. The ε_{eff} is computed from (10) by the direct method followed by the calculation of the approximations A, B_1, and B_2 to ε_{eff} just described.

Realizations of particles consisting of a three-component random mixture are generated in the same way as the two-component particle realizations. Letting f_i, f_w, and f_a be the fractional volumes of ice, water, and air, where $f_i + f_w + f_a = 1$, then a particular 4^3-element subdomain is taken to be ice if the uniformly distributed random number is less than f_i. The region is taken to be water if the random number is greater than f_i and less than $f_i + f_w$, and air if greater than $1 - (f_i + f_w)$. The results are computed for a wavelength of 8.6 mm and displayed in Fig. 6. For the case shown in Fig. 6a, the water fraction f_w is fixed at 0.4 while the ice fraction f_i is varied from 0.1 to 0.6 in steps of 0.1; f_a is then determined from $(1 - f_i - f_w)$. To reduce variability caused by a particular particle realization, the calculations were carried out over five realizations for each value of f_i. The results of the direct method and approximation A are summarized by calculating the mean and twice the standard deviation of the real and imaginary parts of ε_{eff}. One such particle realization, along with the phasor representation of the internal fields, is shown in Fig. 7 for $f_w = 0.4$, $f_i = 0.3$, $f_a = 0.3$. Twice the standard deviations of the imaginary and real parts of ε_{eff} are represented by the lengths of the vertical and horizontal bars for $f_i = (0, 0.1, 0.2, \ldots, 0.6)$. Approximations B_1 and B_2 for ε_{eff} are represented by the symbols "×" and "○," respectively. A second case with $f_w = 0.2$ and $f_i = (0, 0.1, 0.2, \ldots, 0.8)$ is shown in Fig. 6b. Comparisons between the direct method (gray) and approximation A (black) indicate that the agreement for these cases is generally good, although the real part of ε_{eff} from the snow–water approximation tends to be smaller than the value derived from the direct calculation. Generally speaking, approximations B_1 and B_2 are inferior to approximation A: relative to the results

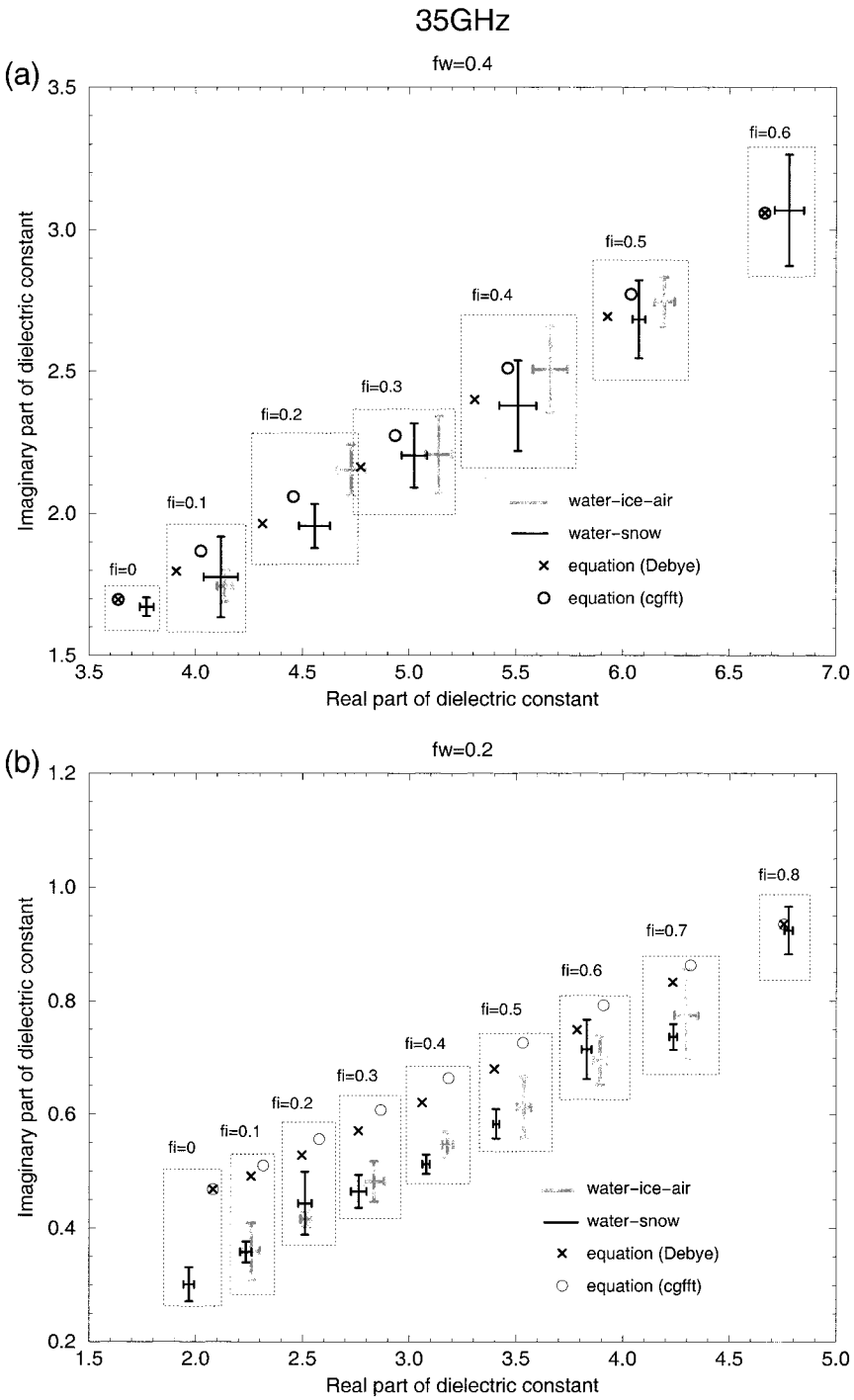

FIG. 6. (a) Estimates of the effective dielectric constant, ε_{eff}, of an air–ice–water mixture with a fractional water volume, f_w, of 0.4 and fractional ice volumes, f_i, of 0, 0.1, 0.2, . . . , 0.6 as derived from direct numerical computations (gray); the water–snow approximation (A) (black); and the two-component approximations using the Debye formula (B_1), and the numerical result (B_2) for the ratio of mean fields in the ice and air. For the direct and water–snow results, the lengths of the sides of the horizontal and vertical bars are equal to twice the standard deviations of the real and imaginary parts, respectively, of ε_{eff} computed from five particle realizations. (b) Same as (a) except that $f_w = 0.2$ where $f_i = 0, 0.1, \ldots, 0.8$.

of the direct method, biases in $\mathrm{Re}(\varepsilon_{\mathrm{eff}})$ occur for $f_w = 0.4$ (Fig. 6a) as well as biases in $\mathrm{Im}(\varepsilon_{\mathrm{eff}})$ for $f_w = 0.2$ (Fig. 6b). The simple analytic expression for $\varepsilon_{\mathrm{eff}}$ provided by approximation B_1 must be weighed against this loss in accuracy.

Before turning to an error analysis of the method, an additional comment should be made. In generating realizations of the mixed-phase particles, the materials are assumed to be uniformly mixed in the sense that the probability of ice, water, or air at a particular location depends only on the corresponding fractional volumes. There are a number of other ways to construct the mixed-phase particles, however, by first combining two of the components and inserting these mixtures into a matrix of the third material. In general, the field ratios for these particle types will not be the same as for the uniformly mixed case.

4. Assessment of errors

The major questions in connection with the mixing formulas given here are their range of applicability and accuracy.

a. Range of applicability

Since the numerical solutions can be carried out only for selected sizes and shapes of the particle and inclusions, it is necessary to specify the range of applicability of the results. Bohren (1986) defines an unrestricted effective medium theory as one that yields functions $\varepsilon_{\mathrm{eff}}$ with the same range of validity as those of substances that are usually taken to be homogeneous (e.g., water). In contrast to this, a restricted $\varepsilon_{\mathrm{eff}}$ can be defined as the dielectric constant of a homogeneous particle that reproduces some or all of the scattering characteristics of a certain class of mixed-phase particles. For the results of $\varepsilon_{\mathrm{eff}}$ presented here, the components of the particle must be randomly distributed; moreover, $\varepsilon_{\mathrm{eff}}$ has been shown to be independent of particle size up to a size parameter of 1. Restrictions on the shape and size of the particle and inclusions can be addressed, in part, by the results of the following calculations:

1) multiple particle realizations using 4^3-element and 8^3-element cubic inclusions,
2) spherical and rod or plate inclusions, and
3) replacement of cubic particle with a spherical particle.

As noted earlier, the results shown in Figs. 3 and 4 were obtained using 4^3-element cubic inclusions where, for each fractional water volume, the mean fields were computed from a single realization of the particle. To examine the variability caused by a change in the particle realization, $\varepsilon_{\mathrm{eff}}$ is calculated for five different particles for each value of f_w where $f_w = (0.1, 0.2, \ldots, 0.9)$ and 0.95 and $\lambda = 8.6$ mm. The results are shown in Fig. 8 where the lengths of the horizontal and vertical

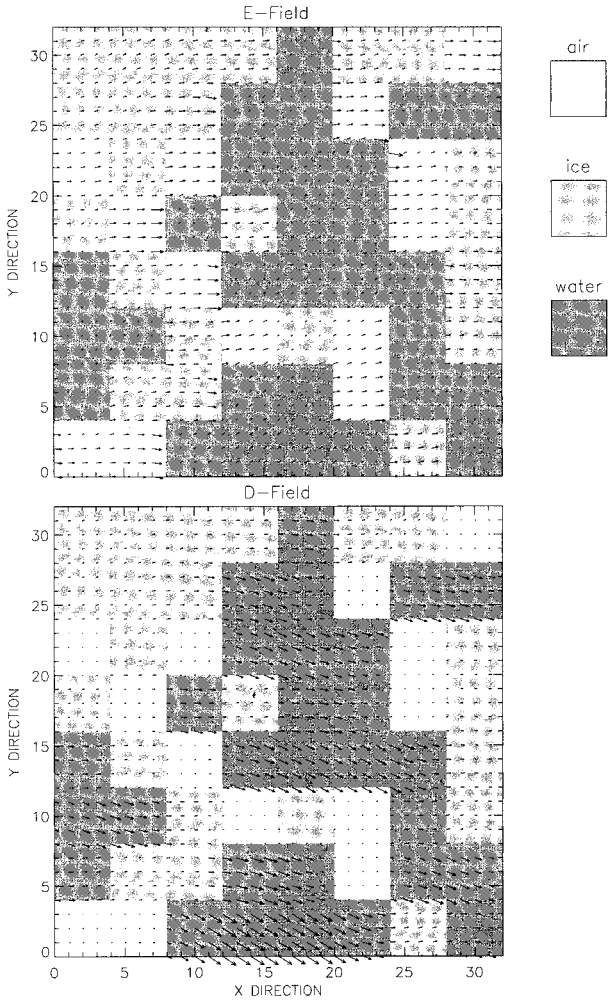

FIG. 7. Same as Fig. 1 but for an air–ice–water mixture. Fractional volumes of the air, ice, and water are 0.3, 0.3, and 0.4, respectively.

bars for each f_w represent twice the standard deviations of the real and imaginary part of $\varepsilon_{\mathrm{eff}}$, respectively. A similar plot is shown in Fig. 8 for particles generated with 8^3-element cubic inclusions. The results suggest that for this range of inclusion sizes (where the 8^3-element and 4^3-element inclusions account for 1/64 and 1/512 of the particle volume, respectively) $\varepsilon_{\mathrm{eff}}$ is relatively insensitive to this parameter and that the fractional water volume is, by far, the more critical variable.

Because the original formulations of Maxwell Garnett and Bruggeman employed spherical inclusions, it is worthwhile testing whether a change from a cubic to a spherical inclusion affects $\varepsilon_{\mathrm{eff}}$. However, because the basic element of the model is cubic, only an approximation for spherical inclusions is possible. An example of this type of particle realization is shown in Fig. 9 where water, of fractional volume 0.3, is taken to be the spherical inclusion material. The regions of water and ice are shown on four successive z = constant planes,

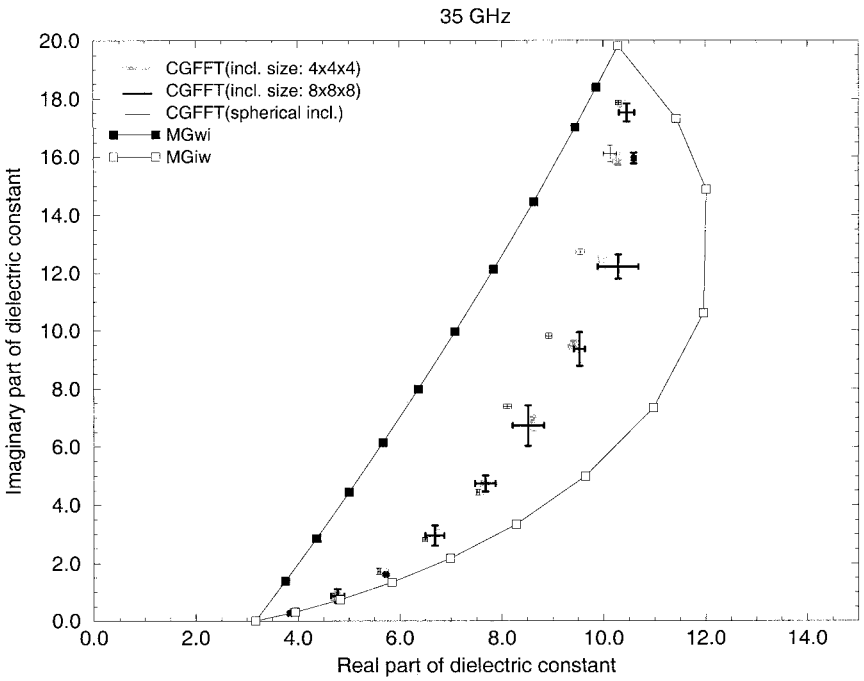

FIG. 8. Comparisons of ε_{eff} for an ice–water mixture for values of the fractional water volume f_w equal to 0.1, 0.2, . . . , 0.9 and 0.95 at a frequency of 35 GHz for cubic inclusions of 4^3 elements (gray), cubic inclusions of 8^3 elements (thick black), and spherical inclusions (black). The lengths of the sides of the cross are equal to twice the standard deviations of the real and imaginary parts of ε_{eff} computed from five particle realizations. Results from the Maxwell Garnett formula are shown for $f_w = 0$, 0.1, 0.2, . . . , 0.9, 0.95, and 1.

where the difference in z from one cut to the next is equal to one element of the grid. It should be noted that because of the way the ''spheres'' are constructed, their fractional volume cannot exceed 0.5 so that for $f_w \leq 0.5$ the spheres are taken to be water in an ice matrix while for $f_w > 0.5$ the spheres are taken to be ice in a water matrix. The results for $f_w = 0.1, 0.2, \ldots, 0.9$, and 0.95 are also shown in Fig. 8. Comparisons to the cases of cubic inclusions plotted in Fig. 8 show that while some discrepancies exist for f_w in the range from 0.6 to 0.8, the agreement is good for $f_w \leq 0.5$ and for $f_w \geq 0.9$.

While the above results suggest that ε_{eff} is not highly sensitive to changes in inclusion size or to a change from cubic to spherical inclusions, based upon the theoretical work of Wiener (1904) ε_{eff} is expected to change significantly if the inclusions are oriented rods or plates. A similar conclusion can be drawn from the results of de Wolf et al. (1990) and Shivola et al, (1989) where a variety of inclusion shapes and orientations are studied. Results of calculations for aligned rodlike inclusions (not shown) confirm that the previous formulas are not applicable to these cases. Nevertheless, based on the results of Bohren and Battan (1986) we expect that if the orientation distribution of the inclusions is random the ε_{eff} would be approximately the same as that derived for the cubic (or spherical) inclusion case. To test this hypothesis within the context of our model, which is presently limited to 32^3 elements, is not possible. It should be noted that particle models consisting of large numbers of elements have appeared in the literature (e.g., Calame et al. 1996).

b. Accuracy

Once ε_{eff} is found from (5), the mixed-phase particle can be replaced by a homogeneous particle of dielectric constant ε_{eff} from which the scattered fields or cross sections can be computed. But since the internal fields of the original mixed-phase particle are known, the scattered fields can be computed directly without recourse to an effective dielectric constant. The accuracy of ε_{eff} can be checked by comparing the scattered fields from these two approaches. A schematic of the test procedure is shown in Fig. 10a. A variation of the test is shown in Fig. 10b where ε_{eff} is obtained from a small mixed-phase particle and then used to characterize the dielectric constant of a larger particle. Next, the small, mixed-phase particle is scaled to the same size as the larger particle and the scattering cross sections from the two particles are compared. This procedure is useful in gauging the range of validity of ε_{eff} as the particle is made larger. An example is shown in Fig. 11 where values of ε_{eff} are derived from (5) using a cubic particle of length on a side of L chosen so that the size parameter, $2\pi r/\lambda$, is equal to 0.1 where r is the radius of an equivolume

sphere. For each water fraction the estimated ε_{eff} is then used to compute the extinction (Fig. 11a) and backscattering cross sections (Fig. 11b) of a cubic particle of size parameter 1 where the results are shown by the triangles at water fractions of 0.1, 0.2, . . . , 0.9. The ''exact'' solution is obtained by scaling the original mixed-phase particle by a factor of 10 and computing the cross sections directly from the internal fields. These data are represented in Figs. 11a,b by the open circles. As with this example, tests at other wavelengths yield good agreement between the two sets of calculations.

The idea of matching the scattering cross sections of the mixed-phase and homogeneous particle can be expressed quantitatively. From the definition of the absorption cross section, σ_a, (Ishimaru 1991) for an incident field of magnitude 1,

$$\sigma_a = k\int \text{Im}[\varepsilon(\mathbf{x}')]|\mathbf{E}(\mathbf{x}')|^2\, dV', \tag{15}$$

where the integral is taken over the volume of the particle. For a mixed-phase particle, the volume integral can be divided into volumes over regions where ε is either equal to ε_1 or ε_2:

$$\sigma_a = k\Bigg\{\text{Im}[\varepsilon_1]\sum_{j\in M_1}\int_{V_j}|\mathbf{E}(\mathbf{x}')|^2\, dV_j' + \text{Im}[\varepsilon_2]\sum_{j\in M_2}\int_{V_j}|\mathbf{E}(\mathbf{x}')|^2\, dV_j'\Bigg\}, \tag{16}$$

where the first (second) summation is taken over all regions of the particle for which the dielectric constant is equal to ε_1 (ε_2). For a homogeneous particle of dielectric constant ε_{eff}, the absorption cross section is

$$\sigma_a = k\ \text{Im}(\varepsilon_{\text{eff}})\int|\mathbf{E}_{\text{eff}}(\mathbf{x}')|^2\, dV'. \tag{17}$$

Although the medium is uniform, the integral can be divided into the same set of subdomains used for the mixed-phase particle so that (17) can be written in the form

$$\sigma_a = k\ \text{Im}(\varepsilon_{\text{eff}})\Bigg\{\sum_{j\in M_1}\int_{V_j}|\mathbf{E}_{\text{eff}}(\mathbf{x}')|^2\, dV_j' + \sum_{j\in M_2}\int_{V_j}|\mathbf{E}_{\text{eff}}(\mathbf{x}')|^2\, dV_j\Bigg\}. \tag{18}$$

Equating (16) and (18), and approximating $\Sigma_{j\in M_k}\int_{V_j}|\mathbf{E}(\mathbf{x}')|^2\, dV_j'$ by $Vf_k\langle|\mathbf{E}_k|^2\rangle$, ($k = 1, 2$) where V is the volume of the particle and f_k is the fractional volume of the kth component, then

$$\text{Im}(\varepsilon_{\text{eff}}) = \frac{\sum_j \text{Im}[\varepsilon_j]f_j\langle|\mathbf{E}_j|^2\rangle}{\sum_j (f_j\langle|\mathbf{E}_{\text{eff}j}|^2\rangle)}. \tag{19}$$

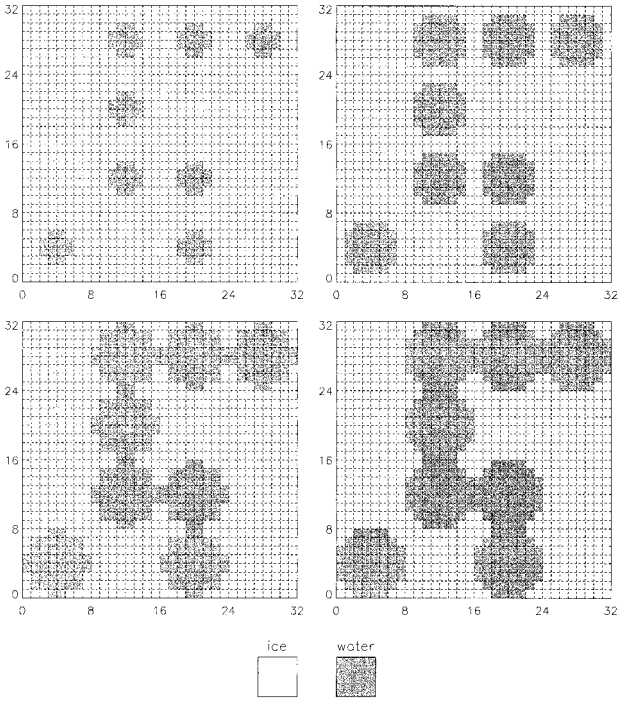

FIG. 9. Example of an ice–water particle mixture with water inclusions, of fractional volume 0.3, that are approximately spherical. The regions of water and ice are shown on four successive z = constant planes, where the difference in z from one cut to the next is equal to one element of the grid.

For an N-component mixture, the summation over j is taken from 1 to N, where f_j is the fractional volume of the jth material and $\langle|\mathbf{E}_j|^2\rangle$ is the mean of the squared modulus of the internal field within this material. A similar expression can be obtained by equating the scattering amplitude (along the direction $\boldsymbol{\theta}$, for example) of the mixed-phase particle to that of the homogeneous particle of dielectric constant ε_{eff}:

$$\varepsilon_{\text{eff}} = \frac{\sum_j \varepsilon_j f_j\langle\exp(jk|\mathbf{r} - \mathbf{r}'|)F_j\rangle}{\sum_j \varepsilon_j f_j\langle\exp(jk|\mathbf{r} - \mathbf{r}'|)F_{\text{eff}j}\rangle}, \tag{20}$$

where

$$F_j = \boldsymbol{\theta}\cdot\mathbf{M}\cdot\mathbf{E}_j \quad \text{and} \tag{21}$$

$$F_{\text{eff}j} = \boldsymbol{\theta}\cdot\mathbf{M}\cdot\mathbf{E}_{\text{eff}j}. \tag{22}$$

The dyadic $\mathbf{M}$ is a function of the observation coordinates, $\mathbf{E}_j$ is the internal vector electric field in region j of the mixed-phase particle, and $\mathbf{E}_{\text{eff}j}$ is the corresponding internal electric field of the homogeneous particle. It is important to note that neither (19) nor (20) provides a direct estimate of ε_{eff} because the denominators are functions of the internal field in the effective medium which itself is a function of ε_{eff}. However, if ε_{eff} is estimated from (5), then the internal fields in the effective medium can be computed. Substitution of these

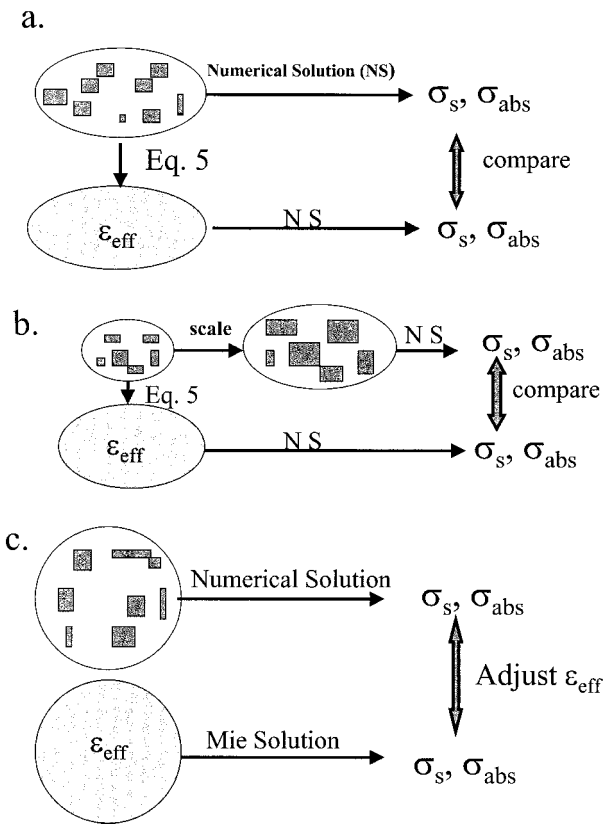

FIG. 10. Schematics of three procedures for checking the accuracy of ε_{eff}.

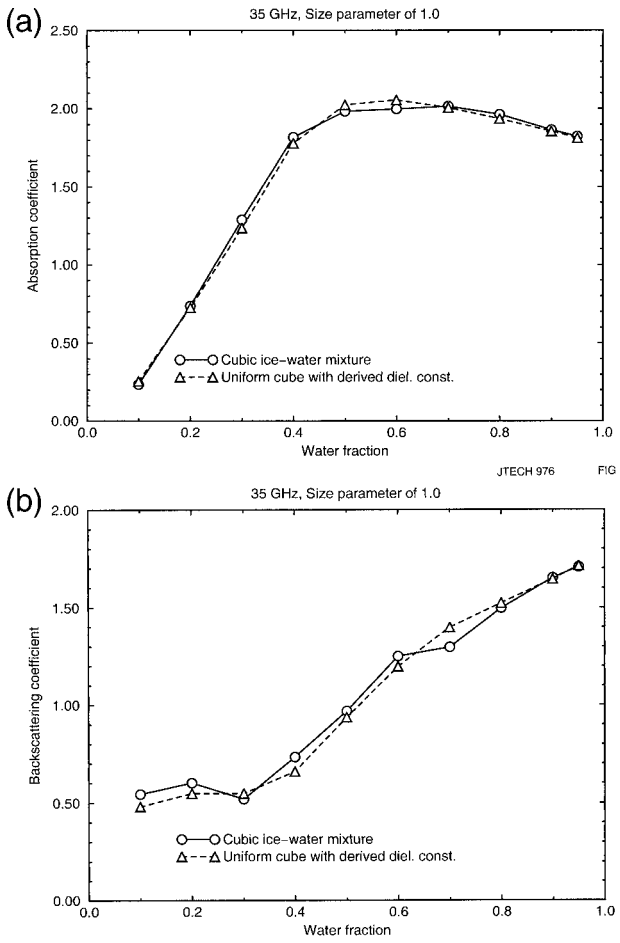

FIG. 11. (a) Backscattering and (b) absorption cross sections vs fractional water volume for cubes of size parameter 1. Triangular data points represent the cross sections obtained by a uniform cube with dielectric constant ε_{eff}. Circular data points represent the cross sections derived directly from the mixed-phase particles. Values of ε_{eff} are derived from mixed-phase particles of size parameter 0.1.

internal fields into (19) and (20) provides numerical estimates of ε_{eff} that are nearly identical to those obtained from (5). If (5) were not used, these equations could be solved iteratively beginning with a replacement of $\mathbf{E}_{\text{eff}j}$ by $\mathbf{E}_j$ in the denominators of (19) and (20).

A somewhat similar approach has been described in a previous paper (Meneghini and Liao 1996) where the scattering cross sections (backscattering and extinction) of a mixed-phase spherical particle are computed using the same numerical method as in this paper. To obtain the effective dielectric constant of the mixture, the scattering cross sections, using the Mie solution, are computed as a function of the dielectric constant of a uniform sphere. The ε_{eff} of the mixture is identified as the dielectric constant which, when used in the Mie calculations, gives the same the scattering cross sections as does the numerical method when applied to the mixed-phase particle. A schematic of this Mie-matching procedure is shown in Fig. 10c. Initial comparisons between this approach and the present method, using (5), showed differences that were traced to two errors. The first arises from an inherent limitation of the numerical method where the spherical particle is approximated by 32^3 cubic elements. This approximation, when used in matching cross sections from the actual (Mie) and approximate spheres, introduces an error in the determination of ε_{eff}, which increases as the fraction of water is increased. The second problem can be traced to a defect in the implementation of the method where the inclusions were allowed to be as small as a single element of the numerical grid. Since the **E** and **D** fields are taken to be uniform within each element, it is not possible to satisfy the continuity of the tangential **E** and normal **D** at the interfaces between the materials. To reduce this error, the minimum inclusion size must be increased so that the inclusions comprise at least 4^3 elements.

These issues can be explored further by means of the numerical results shown in Fig. 12 for ice–water mixtures at a wavelength of 8.6 mm for fractional water volumes, f_w, of (0.1, 0.2, . . . , 0.9) and 0.95. As in Fig. 8, the Maxwell Garnett solutions are shown for reference. Also taken from Fig. 8 are the mean values for a cubic particle with (cubic) inclusions consisting of 4^3 elements (×). For the first set of comparison points,

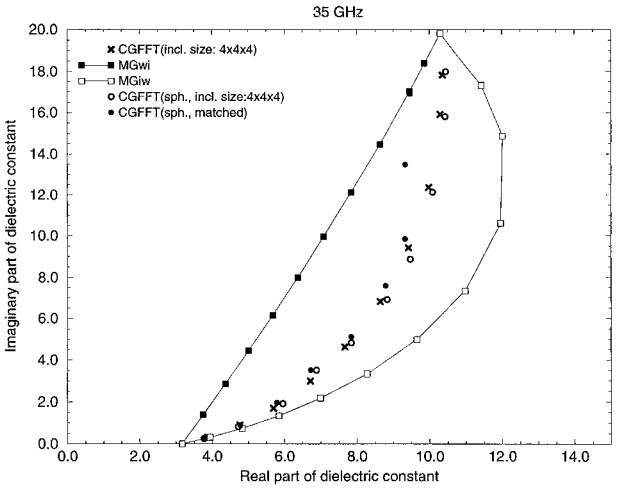

FIG. 12. Comparisons of ε_{eff} for an ice–water mixture for values of the fractional water volume f_w, equal to 0.1, 0.2, . . . , 0.9, and 0.95 at frequency of 35 GHz for (a) cubic particles with cubic inclusions of 4^3 elements ($\times$), (b) spherical particles with cubic inclusions of 4^3 elements (open circles), and (c) same particle realizations as (b) but where ε_{eff} is calculated by means of the Mie-matching procedure (solid circles). Note that the results of (a) are taken from the mean values given in Fig. 8 for the 4^3-element inclusion case.

represented by open circles, ε_{eff} is calculated from a spherical particle with 4^3 element (cubic) inclusions, where ε_{eff} is derived from the internal fields using (5). The good agreement shown between the ε_{eff} derived for both the cubic and spherical particle models suggests that the overall particle shape does not influence the determination of ε_{eff}. As a final calculation, ε_{eff} is computed by matching the scattering cross sections to the Mie solution. The results are represented by the solid circles in Fig. 12. Note that good agreement among the three solutions is found for $f_w \leq 0.7$. For larger f_w values, the Mie-matching solution diverges from the other two. As stated above, the reason for this discrepancy appears to arise from errors in the numerical solutions caused by the imperfect spherical boundary constructed from cubic elements. This source of error is not a factor when calculating ε_{eff} from the internal fields and (5) or from the matching procedure described by (19) and (20) because in these approaches the Mie solution is not used as a reference standard.

5. Discussion and summary

According to (5), the effective dielectric constant, ε_{eff}, of a two-component mixture can be determined from a ratio of the mean fields in the two materials. Using the conjugate gradient method for the numerical solution of Maxwell's equations, ratios of the internal fields were calculated as functions of the fractional water volume f_w, and free-space wavelength λ ($3 \text{ mm} < \lambda < 28 \text{ mm}$) for spatially homogeneous ice–water mixtures. A parameterization in f_w and λ yields a relatively simple expression for ε_{eff}. Calculations of ε_{eff} for air–ice–water mixtures pose a more formidable task because of the introduction of a third variable. Two approximations for ε_{eff} were described: in the first (approximation A), the air–ice mixture is replaced by snow and the two-component version of the formula for ε_{eff} is applied; in the second, the ratios of fields for two component mixtures of water–ice and ice–air are used. The second approximation itself admits of two further possibilities where the ratio of mean fields in the air and ice can be obtained either from the Debye formula (approximation B_1) or by the numerical method (B_2). Comparisons to the numerical results show approximation A to be fairly accurate and generally better than approximations B_1 or B_2. This somewhat offsets the advantage of the B_1 approximation that provides an analytic expression for ε_{eff} for wavelengths between 3 and 28 mm.

To test the range of applicability of the formulas for ε_{eff}, the effects of size, shape, and orientations of the inclusions on ε_{eff} were investigated. A change in inclusion size (from 4^3 to 8^3 elements) or a change of shape from cubic to spherical has a relatively small effect on ε_{eff}. It should be noted, however, that the discrepancies between the spherical and cubic inclusions cases do increase when the fractional water content is between 0.6 and 0.8. On the other hand, calculations of oriented rod inclusions show that the values of ε_{eff} for these cases differ significantly from those derived for cubic or spherical inclusions of the same fractional water volume. Although values of ε_{eff} for eccentric, randomly oriented inclusions are expected to be adequately represented by the formulas given, the particle model used here is not sufficiently flexible to construct particles with spheroidal, arbitrarily oriented inclusions. It is assumed in the calculations that the particle shape (cube) has no effect on the determination of ε_{eff}. This was tested by showing that ε_{eff} as deduced from the internal fields, given by (5), for both spherical and cubic particles produced similar results.

Application of the formulas for ε_{eff} given here for the calculation of the scattering characteristics of melting snow is beyond the scope of the paper. A few comments should be made, nevertheless. One of the primary issues is whether the assumption of a uniform mixing model is appropriate to melting snowflakes, graupel, or hail. In Mitra et al. (1990) snowflake melting is described in four stages. Melting is first manifested as small water drops (tens of micrometers) that form at the tips of the crystal branches. Most of the melting occurs near the boundary and on the lower side of the flake. Later stages include: an inward flow of the melt water augmented by melting in the interior; a change in the structure from one with many small air inclusions to one with fewer, larger inclusions; and finally, a collapse of the ice structure. These observations suggest that while the uniform mixing model might serve as an approximation to the later stages of melting, it is probably inadequate for the initial stage where most of the water is confined to the periphery of the particle. For low fractional water vol-

umes, the scattering properties of snowflakes, graupel, and ice may be more accurately modeled by particles having a dry snow (ice) core and wet snow (ice) coating (Fabry and Szyrmer 1999). If the wet snow or ice mixture can be modeled as a random mixture then the formulas given here are relevant to determining the effective dielectric constant of the mixed-phase outer layer.

Acknowledgments. We wish to thank Dr. Peter Bauer of the German Aerospace Research Institute, Cologne, Germany, for his helpful suggestions.

REFERENCES

Aden, A. L., and M. Kerker, 1951: Scattering of electromagnetic waves by two concentric spheres. *J. Appl. Phys.,* **22,** 1242–1246.

Aydin, K., and Y. Zhao, 1990: A computational study of polarimetric radar observables in hail. *IEEE Trans. Geosci. Remote Sens.,* **28,** 412–422.

Barber, P. W., and S. C. Hill, 1990: *Light Scattering by Particles: Computational Methods.* World Scientific Press, 261 pp.

Battan, L. J., 1973: *Radar Observations of the Atmosphere.* The University of Chicago Press, 324 pp.

Bohren, C. F., 1986: Applicability of effective-medium theories to problems of scattering and absorption by nonhomogeneous atmospheric particles. *J. Atmos. Sci.,* **43,** 468–475.

——, and L. J. Battan, 1980: Radar backscattering by inhomogeneous precipitation particles. *J. Atmos. Sci.,* **37,** 1821–1827.

——, and ——, 1982: Radar backscattering of microwaves by spongy ice spheres. *J. Atmos. Sci.,* **39,** 2623–2628.

Boudida, A., A. Beroual, and C. Brosseau, 1998: Permittivity of lossy composite materials. *J. Appl. Phys.,* **83,** 425–431.

Bringi, V. N., R. M. Rasmussen, and J. Vivekanandan, 1986: Multiparameter radar measurements in Colorado convective storms. Part I: Graupel melting studies. *J. Atmos. Sci.,* **43,** 2545–2563.

Bruggeman, D. A. G., 1935: Berechnung verschiedener physikalischer Konstanten von heterogenen Substanzen: I. Dielectrizitatskonstanten und Leitfahigkeiten der Mischkorper aus isotropen Substanzen. *Ann. Phys.,* **24,** 636–679.

Calame, J. P., and Coauthors, 1996: A dielectric mixing law for porous ceramics based on fractal boundaries. *J. Appl. Phys.,* **80,** 3992–4000.

Catedra, M. F., R. P. Torres, J. Basterrechea, and E. Gago, 1995: *The CG–FFT Method: Application of Signal Processing Techniques to Electromagnetics.* Artech House, 361 pp.

Chylek, P., and V. Srivastava, 1983: Dielectric constant of a composite inhomogeneous medium. *Phys. Rev. B,* **27,** 5098–5106.

——, ——, R. G. Pinnick, and R. T. Wang, 1988: Scattering of electromagnetic waves by composite spherical particles: Experiment and effective medium approximations. *Appl. Opt.,* **27,** 2396–2404.

——, R. G. Pinnick, and V. Srivastava, 1991: Effect of topology of water–ice mixtures on radar backscattering by hailstones. *J. Appl. Meteor.,* **30,** 954–959.

Debye, P., 1929: *Polar Molecules.* Dover, 172 pp.

de Wolf, D. A., H. W. J. Russchenberg, and L. P. Ligthart, 1990: Effective permittivity of and scattering from wet snow and ice droplets at weather radar wavelengths. *IEEE Trans. Antennas Propag.,* **38,** 1317–1325.

Fabry, F., and W. Szyrmer, 1999: Modeling of the melting layer. Part II: Electromagnetics. *J. Atmos. Sci.,* **56,** 3593–3600.

Ishimaru, A., 1991: *Electromagnetic Wave Propagation, Radiation, and Scattering.* Prentice-Hall, 637 pp.

Maxwell Garnett, J. C., 1904: Colours in metal glasses and in metallic films. *Philos. Trans. Roy. Soc. London,* **203A,** 385–420.

Meneghini, R., and L. Liao, 1996: Comparisons of cross sections for melting hydrometeors as derived from dielectric mixing formulas and a numerical method. *J. Appl. Meteor.,* **35,** 1658–1670.

Mitra, S. K., O. Vohl, M. Ahr, and H. R. Prupappacher, 1990: A wind tunnel and theoretical study of the melting behavior of atmospheric ice particles. Part IV: Experiment and theory for snow flakes. *J. Atmos. Sci.,* **47,** 584–591.

Pincemin, F., and J. J. Greffet, 1994: Numerical-simulation of the mean-field in a composite medium. *Physica A,* **207,** 146–150

Sareni, B., L. Krahenbuhl, A. Beroual, and C. Brosseau, 1997a: Ab initio simulation approach for calculating the effective dielectric constant of composite materials. *J. Electrostatics,* **40-1,** 489–494,.

——, ——, ——, and ——, 1997b: Effective dielectric constant of random composite materials. *J. Appl. Phys.,* **81,** 2375–2383.

Sarkar, T. K., E. Arvas, and S. M. Rao, 1986: Application of FFT and the conjugate gradient method for the solution of electromagnetic radiation from electrically large and small conducting bodies. *IEEE Trans. Antennas Propag.,* **AP-34,** 634–640.

Shivola, A. H., 1989: Self-consistency aspects of dielectric mixing theories. *IEEE Geosci. Remote Sens.,* **27,** 403–415.

Stroud, D., 1975: Generalized effective-medium approach to the conductivity of an inhomogeneous material. *Phys. Rev. B,* **12,** 3368–3373.

——, and F. P. Pan, 1978: Self-consistent approach to electromagnetic wave propagation in composite media: application to model granular metals. *Phys. Rev. B,* **17,** 1602–1610.

Su, C. C., 1989: Electromagnetic scattering by a dielectric body with arbitrary inhomogeneity and anisotropy. *IEEE Trans. Antennas Propag.,* **AP-37,** 384–389.

Videen, G., D. Ngo, and P. Chylek, 1994: Effective-medium predictions of absorption by graphitic carbon in water droplets. *Opt. Lett.,* **19,** 1675–1677.

Wiener, O., 1904: ''Lamellare Doppelbrechung.'' *Phys. Z.,* **5,** 332–338.